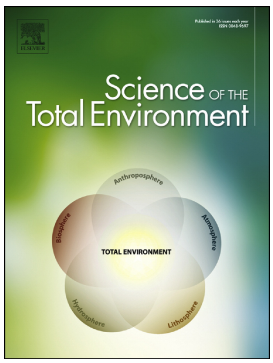

Monitoring the dune-beach system of Guardamar del Segura (Spain) using UAV, SfM and GIS techniques

J.I. Pagán, L. Bañón, I. López, C. Bañón, L. Aragonés

PII: S0048-9697(19)32757-3
DOI: https://doi.org/10.1016/j.scitotenv.2019.06.186
Reference: STOTEN 32840

To appear in: *Science of the Total Environment*

Received date: 11 March 2019
Revised date: 11 June 2019
Accepted date: 12 June 2019

Please cite this article as: J.I. Pagán, L. Bañón, I. López, et al., Monitoring the dune-beach system of Guardamar del Segura (Spain) using UAV, SfM and GIS techniques, Science of the Total Environment, https://doi.org/10.1016/j.scitotenv.2019.06.186

Monitoring the dune-beach system of Guardamar del Segura (Spain) using UAV, SfM and GIS techniques.

Pagán, J.I.[a]; Bañón, L.[a]; López, I.[a]; Bañón, C.[b]; Aragonés, L.[a]*.

[a]Dept. of Civil Engineering, University of Alicante, Carretera San Vicent del Raspeig s/n, 03690 Alicante, Spain

[b]AIRLAB, Singapore University of Technology and Design, 8 Somapah Road, 487372 Singapore

*Corresponding author: Luis Aragonés Pomares. E-mail: laragones@ua.es

ABSTRACT

Dune ecosystems play a key role in coastal dynamics, so it is essential to measure their movements with high precision and monitor their changes over time. It is crucial to have a system that allows us to know the natural and anthropic impacts affecting these ecosystems. The aim of this study is to ascertain the historical evolution of the dune system of Guardamar del Segura (Spain) and its relationship with coastal erosion. Likewise, it is also intended to assess the state of the foredune restoration works carried out in 2011. To this end, a comparison of existing cartographic data has been undertaken by using geospatial analysis techniques through Geographic Information Systems (GIS). As a novelty, a low takeoff weight UAV (Unmanned Aerial Vehicle) has been used to produce a high-precision 3D model from two-dimensional images using photogrammetric techniques, such as Structure from Motion (SfM). This technique made it possible to obtain a digital terrain model of high density and precision (30 pt/m^2 and RMSE Z of 0.173 m). The results show a constant erosion of both the beach and the foredune, with an overall loss of 143,561 m^3 of material in the period analyzed (2001-2017). The anthropogenic restoration actions executed within this period have not been

effective. In fact, erosion has increased in the period 2016-2017, with a significant reduction in the beach width and sea waves directly affecting the foredune. The main conclusion is that the combined use of UAV and SfM techniques is an excellent procedure to periodically supervise dune ecosystems with high precision and significant time and cost savings.

Keywords: dune erosion, UAV, SfM, DEM, shoreline evolution, GIS.

1 INTRODUCTION

An accurate knowledge of the beach-dune ecosystem is essential, as it is a dynamic area where terrestrial and marine ecosystems interact. These natural interactions can be altered by human action, modifying coastal dynamics, causing alterations in beaches and dunes, and affecting their stability (Bird, 1985; Burak *et al.*, 2004). Dunes are a significant part of the coastal system. Wind plays a primary role in their genesis, in those coastal zones where the sea makes a contribution of sediments that come from the transport of river courses and littoral drift (Aldeguer, 2008). These coastal dunes, developed on coasts with an arid climate, constitute a unique biotope due to the interaction between terrestrial and marine ecosystems. In addition to the effect on terrestrial biocenosis, waves and wind erode or deposit, transport or abandon materials, in a highly dynamic way, modifying not only the coastal area but also affecting terrestrial ecosystems (Carter *et al.*, 1990). It is essential to know the evolution of those dune systems in which backshore erosion has led the affection of the foredune by waves during storms.

These natural interactions are also influenced by human actions, such as the construction of buildings close to beaches and promenades, as well as the direct interaction of breakwaters and ports (Aragonés *et al.*, 2016; Halpern *et al.*, 2009; Steffen *et al.*, 2007). All these factors may modify coastal dynamics and transport of sediments, altering the shoreline and affecting the stability of the beaches (Pagán *et al.*, 2016). Disturbances start on the nearshore due to discrete or gradual events of variable space-time intensity, such as wave impacts, seawater floods, erosion, or sand sedimentation, which afterward will reflect in the stability of the backshore and the foredune (Hesp and Martínez, 2007).

A possible method to evaluate the dune system is by means of its morphological changes. This practice is acknowledged by researchers and provides a detailed vision of the changes produced in the shoreline (Komar, 1983). For this, it is necessary to determine the increase or

decrease of sediment volumes for specific parts of the coastal system –beach and foredune— that explain what is happening in the backshore. When these differences are known, an assement can be done to establish whether the system is gaining or losing sediment volume. In addition, when this assessment involves subzones within a larger system, it is possible to identify where additions and losses of sediment are occurring. Applying this approach to the monitoring of beach nourishment projects would provide useful information about the redistribution of fillings from the nourished area to adjacent areas (Ley *et al.*, 2007).

Coastal dunes are difficult to study because of the complex interaction between topography, bathymetry, vegetation and wind and coastal processes that move sand throughout the entire system. To monitor changes on the dune system, it is necessary to repeatedly measure their topography over time. Collecting accurate data using classical topographic surveys is labor-intensive and time-consuming, even using modern techniques such as real-time kinematic Global Navigation Satellite System (GNSS) surveys (Andrews *et al.*, 2002). Although the use of transects seems to be acceptable in the case of a linear and consistent feature such as a beach, when the topography becomes more varied (as in a dune area), the ability for one or more transects to accurately represent a wide area decreases (Mitasova *et al.*, 2005). In addition, accurate volumetric measurements are difficult to obtain due to the low resolution of the collected data. Laser Imaging Detection and Ranging (LIDAR) deployed on aircrafts flying at low altitude has been shown to provide accurate horizontal and vertical measurements (Woolard and Colby, 2002). Several studies have demonstrated the ability of LIDAR data to accurately represent topography in large coastal areas (Revell *et al.*, 2002; Sallenger Jr *et al.*, 2003), and LIDAR sequential surveys have shown that coastal changes can be monitored over time (Stockdon *et al.*, 2009). However, the high cost of these flights makes that their collection often depends on government-sponsored flights, which affects the temporal coverage of available data (Andrews *et al.*, 2002).

In the last years, the emergence of affordable unmanned aerial vehicles (UAV) for civil uses, along with the development of image-based computing techniques such as structure from motion (SfM), has dramatically increased UAV-based photogrammetry to produce high resolution terrain models for the study of different surface processes (Colomina and Molina, 2014). This emerging technology can be also combined with other existing methods, such as GNSS, terrestrial laser scanner (TLS), satellite or aerial remote sensing imagery (Elsner *et al.*, 2018).

UAV-based photogrammetry has several advantages in comparison with the methods mentioned before. It allows the study of specific areas with short high-performance field surveys and the desired frequency in data acquisition, obtaining good quality results. Current applications of UAV in natural environments include landslide monitoring (Lucieer *et al.*, 2014; Niethammer *et al.*, 2012), fluvial dynamics (Javernick *et al.*, 2014; Miřijovský and Langhammer, 2015), bank erosion (Prosdocimi *et al.*, 2015), vegetation monitoring (Dandois and Ellis, 2010; Jaakkola *et al.*, 2010), and coastal environment surveying . In this field, previous research has demonstrated that UAVs are appropriate for precision topographic surveys and for monitoring surface changes over time. Delacourt *et al.* (2009) developed an unmanned photogrammetric helicopter equipped with autopilot system in order to obtain a high-resolution digital elevation model (DEM) of a French beach. (Mancini *et al.*, 2013) proved that the elevation data obtained using UAV-SfM methods had a similar accuracy as those acquired using TLS surveys in a beach dune system located at Ravena (Italy). Drummond *et al.* (2015) described several coastal engineering and management UAV applications, including rapid pre- and post-storm UAV deployment for quantifying coastal impacts of a major storm event that struck Sydney in April 2015. Gonçalves and Henriques (2015) stated that UAVs can replace the conventional aerial surveys carried out in current coastal monitoring programs, with a considerable reduction in data acquisition costs while maintaining the quality of topographic and aerial imagery data. Long *et al.* (2016) used UAV imagery to monitor the topography of a dynamic tidal inlet on the

Atlantic French coast. Turner *et al.* (2016) deployed UAVs to monitor and evaluate the post-storm dune and beachface spanning along a coastal embayment. Chen *et al.* (2018) performed high resolution UAV topography on a beach in the Taiwan strait, monitoring its changes over time and improving the quality of vertical DSM data. Scarelli *et al.* (2016) proposed the use of low-cost UAVs to monitoring the dune system, and Scarelli *et al.* (2017) used UAV flights to monitor the changes on the beach-dune system by anthropogenic and natural factors.

This research studies the coast of Guardamar del Segura, Alicante (Spain), strongly affected by anthropogenic pressure and beach erosion (Pagán *et al.*, 2017). The aims of this paper are: (i) to analyze the evolution of the dune-beach system evaluating the dune erosion caused by the regression of the shoreline. (ii) to evaluate the effects of the restoration of the foredune ridge carried out in 2011 and (iii) to assess the applicability of UAVs to carry out periodic precision surveys at a reasonable cost. The methodology provided can be used to study and protect the threatened coastal dune systems.

2 MATERIALS AND METHODS

2.1 STUDY AREA

2.1.1 Environmental settings

The great dune system of La Mata-Guardamar covers the beaches to the north and south of the mouth of the Segura River (Figure 1), with a total length of more than 11 km of coastline. Its development was able due to the optimum environmental conditions: proximity of the Segura River which has provided sufficient solid sediment supply to the shore, depositional coast whose beach has acted as a source of sand supply, scarce vegetation cover which has allowed the mobility of the sand and a favorable wind regime (Matarredona Coll *et al.*, 2006). The scope of this study focuses on the foredune ridge of the coastal area that extends from the north of the town of Guardamar del Segura (Alicante) (Figure 1c), specifically a 1,500 m stretch from the so-called Casas de Babilonia, to the mouth of the Segura River, the Viveros beach.

This is a dissipative beach, has 45 m width on average and is formed by fine golden sands with a median size D_{50} of 0.228 mm.

The foredune has three sections with well-differentiated typologies (Figure 1d):

1. The first zone is located at the northern end of the study area, next to the mouth of the Segura river. This section has a profile that has been completely altered by the dumping of materials dredged from the construction of the marina. A wall has formed, with a trapezoidal section, between 4.5 m and 8 m high, a lower base about 72-73 m, and an upper base of from 43 to 53 m wide of compact materials that are unrelated to the texture and natural cohesion of the dunes.

2. A second central zone where the dune advances inland and has a more level and extended slope, which is over 63 m wide, with a height of only 2.9 m.

3. A third zone to the north of Casas de Babilonia, where the dune has a very steep slope towards the sea, with its advance inland being contained by a wall of vegetation (mainly eucalyptus and acacias). The dune here has a considerable height, about 4.5-5 m high for a width of 46 m.

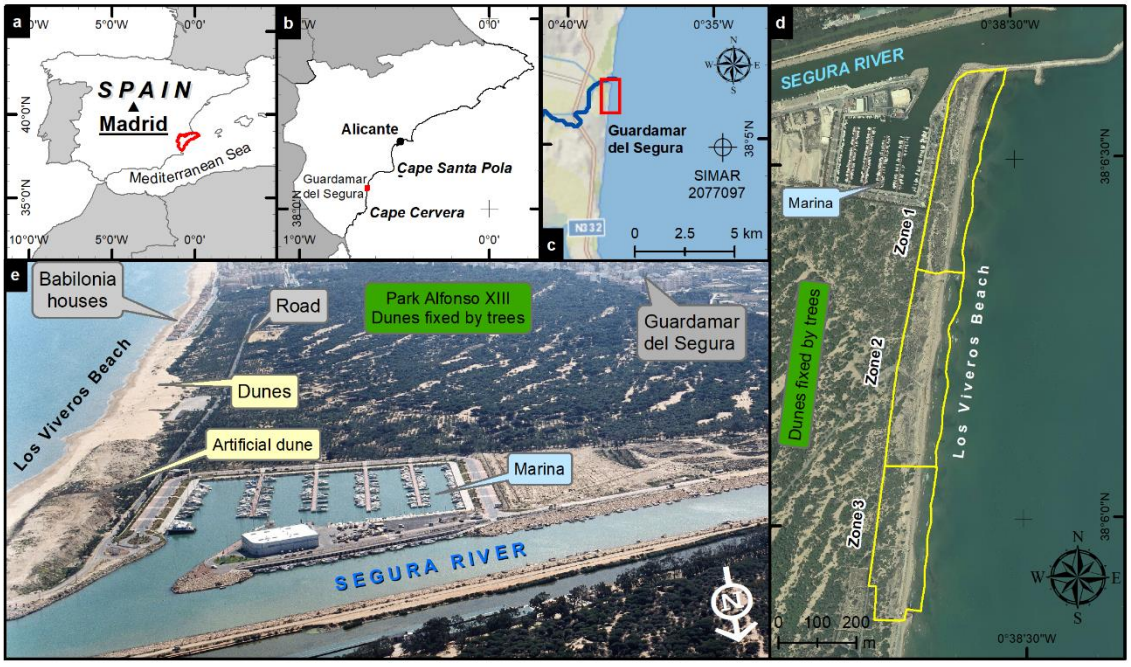

Figure 1: (a) Study area located in Spain, (b) in province of Alicante and (c) in Guardamar del Segura town, with location of the SIMAR node used for wave data. (d) Location of beaches and significant elements on the coast of Guardamar del Segura. (e) Aerial image of Segura river mouth (MAPAMA, 2017).

2.1.2 Coastal dynamics

Pagán *et al.* (2017) studied the influence of coastal dynamics on the evolution of the shoreline of the study area for the period 1956-2014. The direction of the mean flow is N90.3°E, while the coast has an orientation of 8° with respect to N. This causes the direction of the longitudinal transport of sediments to be N-S (Figure 2a). In addition, the length of the breakwaters at the mouth of the Segura reaches the DoC causing the longitudinal transport to be cut. This makes the transverse transport of sediments prevail, causing a greater retreat along the shoreline. The tidal range is negligible, only influenced by meteorological conditions, with values oscillating around 0.3 m (Ecolevante, 2006).

Regarding the incident waves, the most frequent (40%) are those in the E direction, followed by the ENE and ESE, with no relevant differences between periods (Figure 2b). The most energetic storms are those of NE direction. Observing the time series (Figure 2c), no increase in the frequency or intensity of the storms has been detected, although there are fewer storms whose wave height exceeded 3 m in the period 2001-2009 than in the rest of the periods. The highest number of storms occurred in 2014 and 2015, exceeding 4.5 m. Between Nov-2016 and Apr-2017 there were 4 storms whose waves exceeded 3 m and which seriously affected the dwellings located in the adjacent area, as studied Pagán *et al.* (2017).

The predominant wind direction are the NE and ENE (Figure 2b), so the predominant wind transport is towards the coastal interior. A slight increase in both frequencies and speeds has been detected in recent years, with speeds of about 10 m/s maximum.

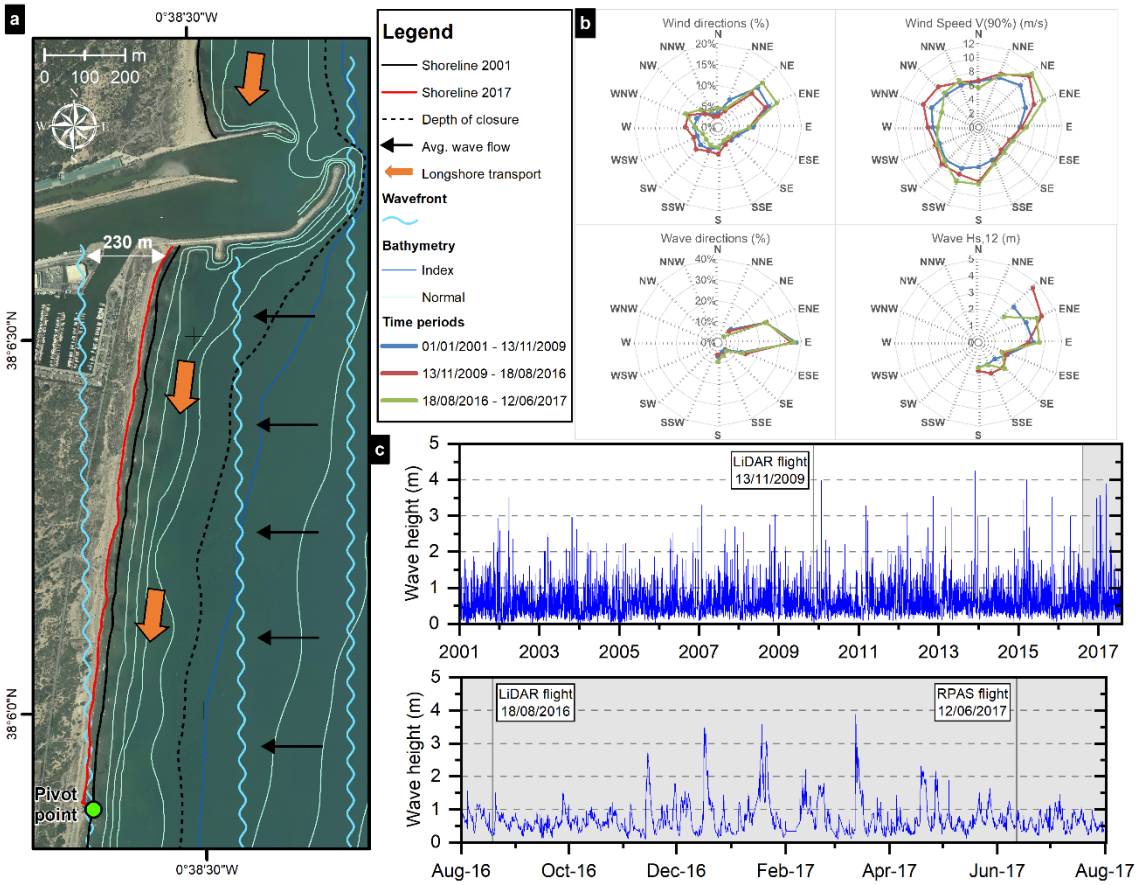

Figure 2: (a) Littoral dynamics (b) Wind and wave roses (c) Wave height for the complete period of study.

2.1.3 Anthropogenic stress

The study area is subject to a tremendous anthropogenic stress, not only from the residents of Guardamar, but also from people coming from neighbouring towns and holliday housing estates. Moreover, that area has experienced strong urban growth, and it is especially crowded in summer, when the ecosystem is more fragile. All this activity has progressively altered and destructed the psammophilous communities, as well the forest and bush species, due to trampling and, to a lesser extent, litter dumping (Aldeguer, 2008).

A marina was built in 1998 on the mouth of the Segura river (Figure 1e). An approximate volume of 200,000 m^3 of sediments were dredged (Aldeguer, 2008) and dumped to create an artificial dune between 4.5 and 8 m of height. According to the geotechnical, these materials were basically sands, with a low proportion of silts (Matarredona Coll *et al.*, 2006). It is also

possible to notice the emergence of plant species typical from nitrogenated or halomorphic soils, that are slowly being replaced by psamophilic species. (Matarredona Coll *et al.*, 2006).

A restoration to recover the foredune from the different aggressions it was suffering was planned in 2002 and finally completed in 2011 (MAPAMA, 2001). The actions executed were the following:

1. In the Zone 1 of the project area, the aim was to completely eliminate the previously dumped anthropogenic materials dredged from the marina site, exposing the sands of the existing dune, and proceed to planting with autochtonous species to fix it.

2. In the Zone 2, the proposed solution was to attempt to stop the dune progression and fix it by seeding –also using protective barriers— with the typical flora of this environment.

3. In the Zone 3, the dune was kept in its current shape, leaving the supporting trees (eucalypts and acacias) at the front of the dune, thereby eliminating the presence of knife grasses and pitas on the dune, and seeding it to naturalize and stabilize it.

2.2 METHODS

The methodology followed in this study is summarized in Figure 3.

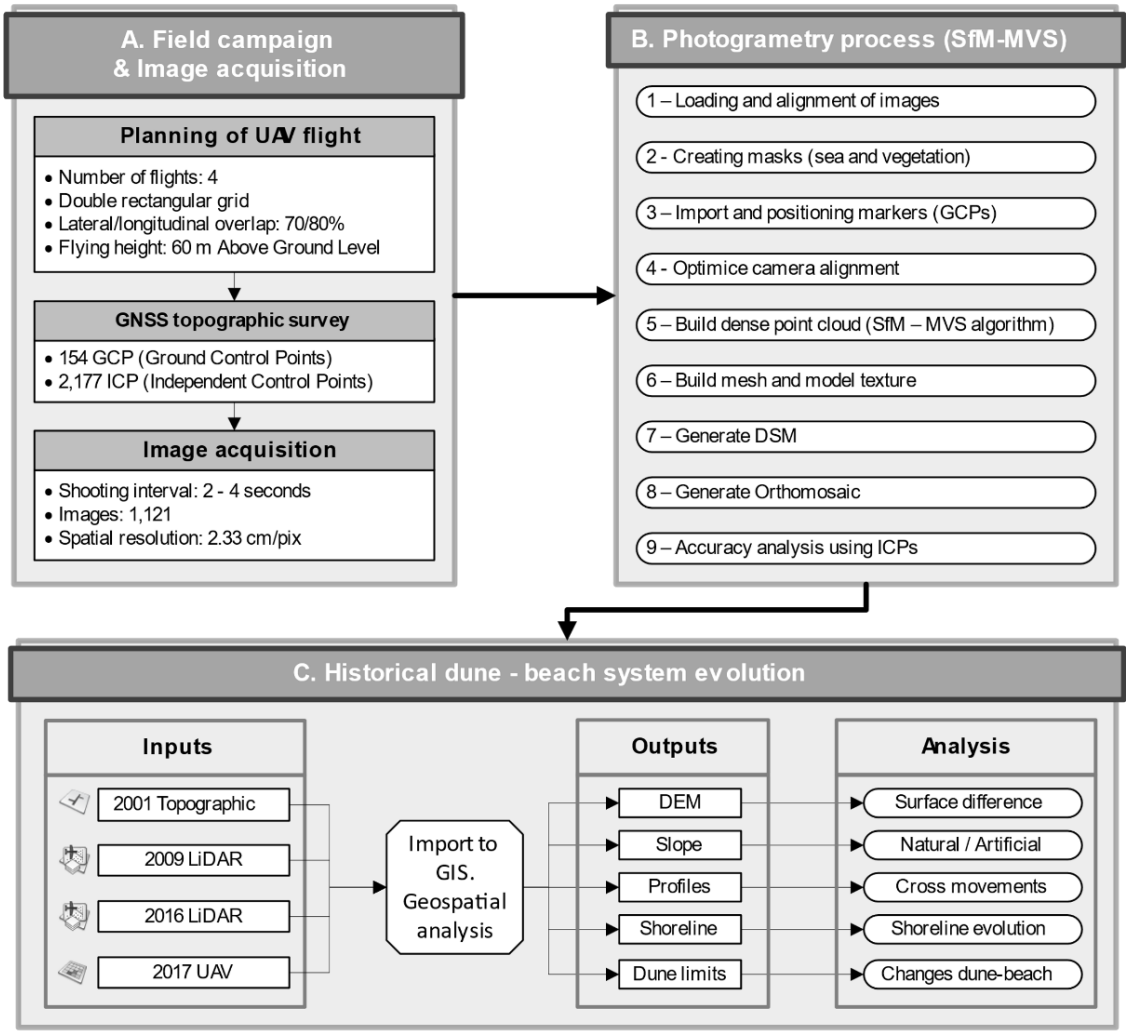

Figure 3: General workflow followed, from (A) the field campaign and image acquisition, (B) the photogrammetry process of the images using SfM-MVS algorithm and (C) the historical dune-beach system evolution analysis using geospatial GIS techniques.

2.2.1 Field campaign and data acquisition

The field campaign took place on June 12, 2017. A DJI Phantom 4 quadcopter was used for the acquisition of the aerial images (Supplementary data 1d). The UAV is equipped with a built-in camera FC330 and a 1/2.3" CMOS sensor (12.4 Mpixel resolution). The lens has a Field Of View (FOV) of 94º 20 mm (35 mm format equivalent) f/2.8 focus at ∞. Its 6,000 mAh smart battery allows an effective flight time of approximately 20 minutes per charge. For the mission planning, the free application Pix4DCapture was used (Pix4D, 2019), according to the operating parameters indicated in Figure 3a. Since the purpose of this campaign was a 3D reconstruction

of the terrain, the flight path was set in a double mesh configuration (longitudinal and lateral), allowing to overlap the aerial photography, which is indispensable for the creation of 3D model through SfM approach, taking images at intervals between 2-4 s at a flying altitude of 60 m (Supplementary data 1a,c and 3). The weather conditions were adequate, the wind speed was weak and uniform, with no gusts, so the flights were performed as planned.

2.2.2 Ground control points and GNSS Surveys

Ground control points (GCPs) are necessary for an accurate georeferencing of the aerial images and the derived point cloud model. For this reason, a total of 154 GCPs were acquired using a Leica Viva GS16 GNSS receiver. This device was connected to the GNSS reference station network of Valencia (ERVA network) via GPRS/3G connection and used Real time Kinematic (RTK) with network solution to acquire the coordinates in datum ETRS89, obtaining an accuracy of ±2 mm in both planimetry and altimetry. With the network solution the distance to the nearest station is not considered, but the receiver must be within the area of the triangles defined by the stations, which is this case.

Artificial targets were used as GCP, deploying white paper sheets on the ground, partially buried to protect them from the breeze. Once CGPs were positioned, the coordinates of each center were taken (Supplementary data 1e). GCPs were distributed along the study zone, with the purpose that at least 2 of them were visible in every image taken from the UAV. To evaluate the vertical and horizontal errors, complementary GNSS measurements were made. A total of 2,177 independent control points (ICPs) were surveyed (Supplementary data 2a). All the data were acquired using the UTM WGS84 coordinate system.

2.2.3 SfM-MVS based photogrammetric process

The photogrammetric process based on Structure from Motion (SfM) together with multi-view stereo algorithms (MVS) allows the reconstruction of the coastal topography in 3D from 2D images. The SfM-MVS algorithm generates the geometry of the scene, processing the different

positions and orientations of the cameras from a set of multiple overlapping images (Snavely *et al.*, 2008). A commercial software, Agisoft PhotoScan (Agisoft, 2016), was chosen for this study due to its essentially automated process, based on multiview 3D reconstruction technology, and its suitability for UAV image processing. The complete workflow consists of 9 steps (Figure 3b).

In the first step, the images taken from the UAV flight were uploaded. Information regarding focal length, sensor and camera positions is gathered automatically from images' EXIF metadata. This information contains the coordinates of the GNSS signal received by the UAV and its orientation. In the PhotoScan alignment process, coincidence points between overlapped images are detected, obtaining the actual camera position for each image and correlating the images one another. Although image distortion is small, for photogrammetric processing camera calibration parameters need to be set very precisely. By default PhotoScan software performs auto calibration during image alignment/optimization and estimates required calibration coefficients automatically. This process provided a scattered point cloud along with the position and relative orientation of the aerial images. The second step was the manual masking of the water zones corresponding to the sea and to tall vegetation.

The third step consisted of importing and positioning the markers. These markers are used to optimize camera positions and orientation data, obtaining better model reconstruction results. In addition, the DSM will be thus geoferenced, which will allow its integration into a GIS for later analysis along with other layers of geographic information. For this reason, this stage consists of locating the GCPs visible in each photo and placing a marker in the corresponding point of the image. This is a semi-automatic process because although the software automatically identifies the position of the markers in each related photo, it is necessary for the user to make a precise adjustment to

provide maximum accuracy. This step is the most time consuming. Finally, the coordinates of the 154 surveyed GCPs are imported from a file.

The fourth step is to optimize the camera alignment. The position of the images is recalculated taking into account the set GCPs, so that the resulting point cloud will be accurately georeferenced in XYZ coordinates. In the fifth step, the software calculates the depth information for each camera using the MVS algorithm, generating a single dense point cloud coloured in RGB scale. Once the dense point cloud has been reconstructed, it is possible to generate a polygon mesh model (sixth step) based on the dense cloud data. If necessary, some obvious outliers and points with large projection errors are checked and removed manually, and then the optimization process is repeated.

The final result can be exported both as DSM raster (seventh step) and orthophoto (eighth step), using UTM ETRS89 H30N (EPSG 25830) projected coordinate system in GeoTIFF format. A total of 1,121 images were processed, covering a surface area of 286,100 m^2. The whole SfM-MVS computing process took a total time of 33 hours. Detailed information about the results of the SfM-MVS process for each zone is shown in Supplementary data 3.

The average spatial resolution in the UAV images is 2.25 cm/pixel. With this high resolution, a dense point cloud was constructed with more than 8 million points, generating a polygonal mesh from which a DSM with a density of 32 points per m^2 was derived (Figure 4e). This high point density allows the dune shapes to be modeled with great accuracy (Figure 4f). From the DSM and the aerial images, an orthophoto with a spatial resolution of 5 cm/pixel was generated, making it possible to visualize even the smallest detail of the study area, including the beach users' footprints on the sand (Figure 4a-d). From the combination of DSM and orthophoto, a realistic 3D model of the dune-beach system can be generated for analysis from different points of view (Figure 4g).

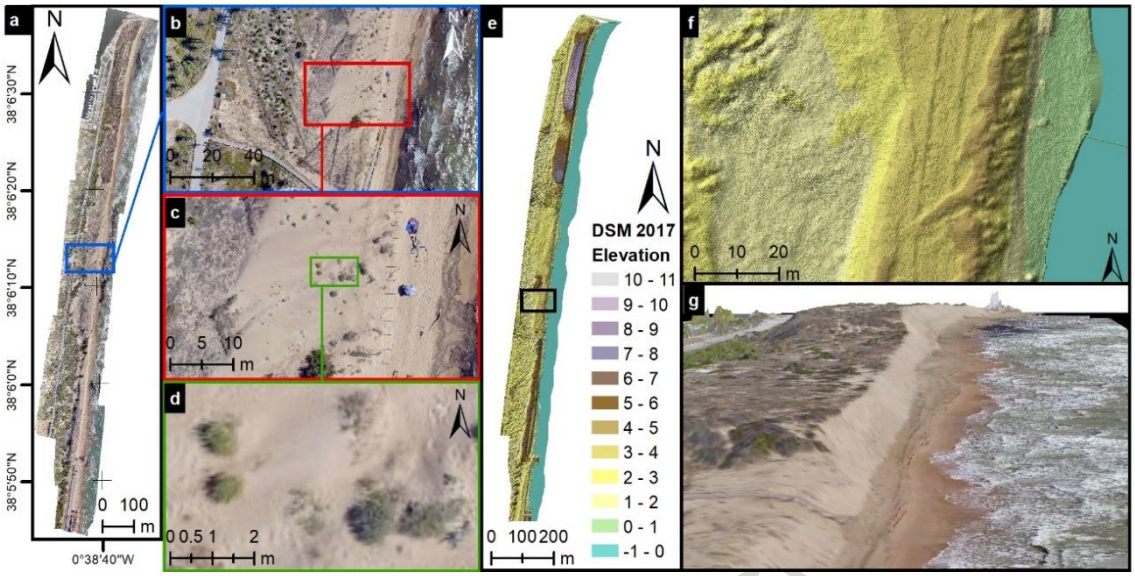

Figure 4: (a) Orthomosaic image of the area of study with a spatial resolution of 5 cm/pix. (b) Zoom at 1:5000 scale. (c) Zoom at 1:1000 scale (d) Zoom at 1:100 scale. Footprints on the sand can be distinguished. (e) DSM of the area of study. (f) detail of the DSM, where the high precision in the modelling of the dune is appreciated. (g) detail of the realistic 3D model using the DSM and orthomosaic.

154 GCPs were used for the georeferencing process of the model. The validation of the SfM-MVS model (ninth step) was calculated using 2,177 ICPs collected during the GNSS precision survey. Focusing on the analysis of altimetric accuracy, Supplementary data 2 shows the dispersion in the measurement between the 3D model obtained from the UAV and the validation set surveyed with GNSS. A linear fit between GNSS and DSM from UAV vertical measurements is obtained, with a R^2 above 0.98 and a Root Mean Squared Error (RMSE) of 0.173 m. In addition, the RMSE Z from the different types of surfaces of the study area has been calculated. The RMSE Z in the dune area is 0.136 m whereas in the beach is higher, 0.195 m for Backshore and 0.222 m for Wet Sand. Road (0.083 m) is the lowest and Walkways is the highest with a RMSE Z of 0.231 m. The planimetric RMSE (XY) was 0.07 m for the whole area of study and below 0.10 m for each surface.

2.2.4 Historical evolution of the dune-beach system

The next stage comprised the historical analysis of the evolution of the dune-beach system (Figure 3c). For this study, in addition to the DSM generated in the previous section, the contour map from the topographic survey carried out in 2001 by the Directorate General of Coasts from the Spanish Ministry of the Environment (MAPAMA, 2001), the raster 1-meter DEM obtained from the LiDAR flight of the 2009 (PNOA, 2009) and the digital files of point clouds belonging to the 2nd LiDAR Coverage of the 2016 with true color (RGB) (PNOA, 2016) were also used. Both DEMs are part of the PNOA (Plan Nacional de Ortofotografía Aérea) governmental surveys and available for public download under license CC-BY 4.0. Their main characteristics are shown in Supplementary data 4.

In order to perform geospatial analysis such as DEM comparison, sediment change maps or cross-shore transects it is necessary to incorporate the datasets into a GIS environment. In this research, the ArcGIS 10.5 software with the 3D Analyst extension (ESRI, 2016) has been used. Given the diversity of formats in which the data are provided (vector, raster, LAS point clouds) the first step involved the creation of a terrain dataset for each date. A terrain dataset is a multi-resolution TIN-based surface created from measurements stored as entities in a geodatabase. The slope of the surface, expressed in sexagesimal degrees, is generated from the DEM, allowing to analyze if the present slopes correspond to the natural slope (when slope is below than the friction angle of sand, 35º). If is higher, it means that it can be caused by anthropogenic actions. An advantage of using DEMs is that it is possible to interactively generate cross-shore transects anywhere in the study area for each date studied. The position of the shoreline and the foot of the dunes is also identified. Shoreline for the UAV DSM has been manually delineated using the orthophoto generated. The criteria to identify the shoreline was marking the high-water mark on the beach. Also, for the foot of the dune, the line was delineated by the combination of visual identification on orthoimages and changes in the slope of the DSM. Finally, changes were detected between the 3 available time periods

(2001-2009, 2009-2016 and 2016-2017) as well as within the total study period (2001-2017). The volumetric difference between two DEMs was calculated using the ArcGIS Surface Difference tool. The ArcGIS Surface Volume tool was used to obtain the volume above elevation 0.

2.2.5 Soil sampling and sedimentological study

There are sediment samples located in 8 representative sections of the dune and the backshore, belonging to the 2006 field campaign (Ecolevante, 2006). In order to identify changes in sediment composition, in the new 2017 campaign samples were collected in exactly the same locations as in the previous campaign. All the samples were subjected to a granulometric analysis (UNE 103 101:1995, UNE 7050-2 and UNE 103 100), characterizing the sediment by its median size (D_{50}) and textural parameters (asymmetry, kurtosis and classification).

3 RESULTS

The changes on the coastal system has been investigated by the combined analysis of high-resolution DSM from UAV survey and previous DEM from LiDAR and topographical surveys using GIS surface analysis techniques.

3.1 Dune-beach system evolution

Figure 5a-d shows the shaded topography of the foredune, identifying the 3 different zones described in section 2: zone 1 with a trapezoidal shape up to 10 m high; zone 2 with the least developed foredune and zone 3, identifying a foredune between 5 and 6 m high just on its boundary with the beach. In the area between the foredune and the road is flat with heights between 1 and 2 m. An interesting analysis to be made is the evolution of the slope maps over time (Figure 5e -h). A progressive increase of the slopes on the sea side of the dune throughout the study area is detected. The color scale has been adjusted in order to identify the areas with a slope greater than the angle of friction at rest of the sand. In this respect,

zone 1 shows slopes exceeding 35° on both sides (sea and land side) and that as time goes by, the slope increases, reaching the entire length of the coastal front by 2017, with values even greater than 45°.

This situation of increase in the slope of the seaside of the dune is repeated in zone 3, where it goes from slopes of less than 26° until 2009 to slopes of up to 30° in 2016. Moreover, in 2017 a significant increase in the slopes of the coastal front of that area is detected, with red colors appearing indicating slopes greater than natural ones. It should be noted that on the land side the slope of the dune remains between 27-30°. In zone 2 there is also an increase in the slope from 2001 to 2017, although the values in this section are below 30°, indicating that the reconstructed profile is similar to the original natural profile.

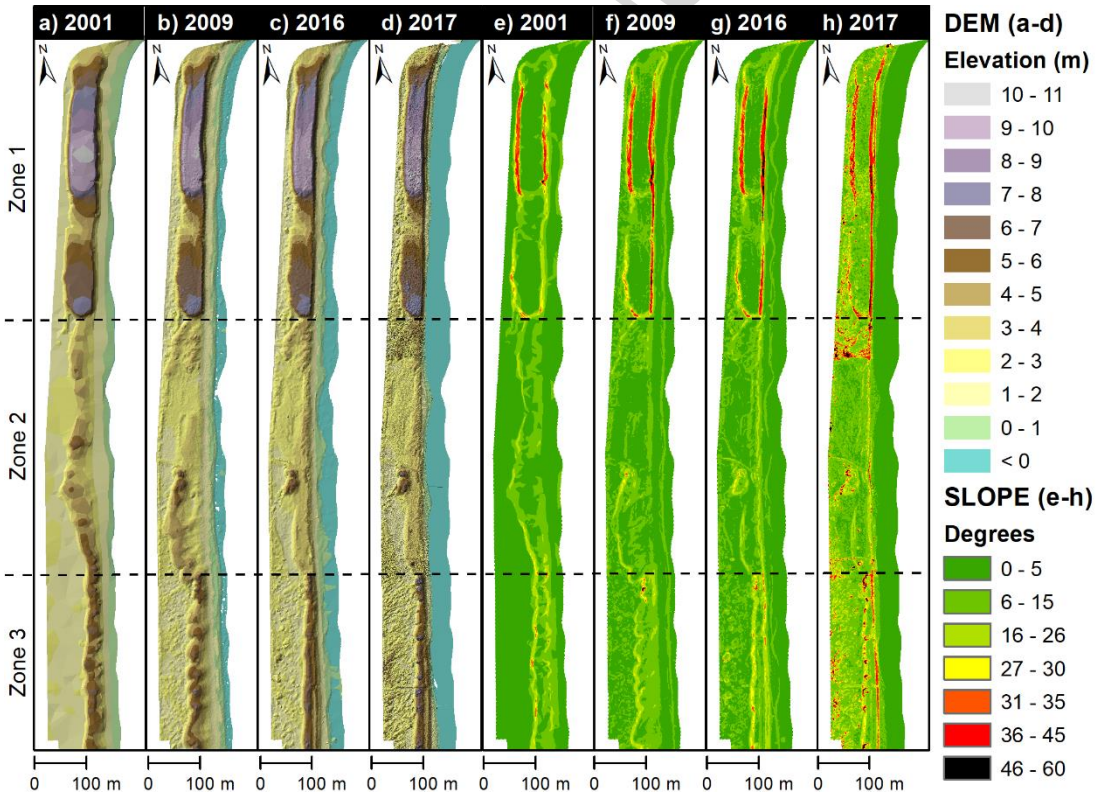

Figure 5: Digital elevation models (DEMs) (a-d) and slope (e-h) in each date.

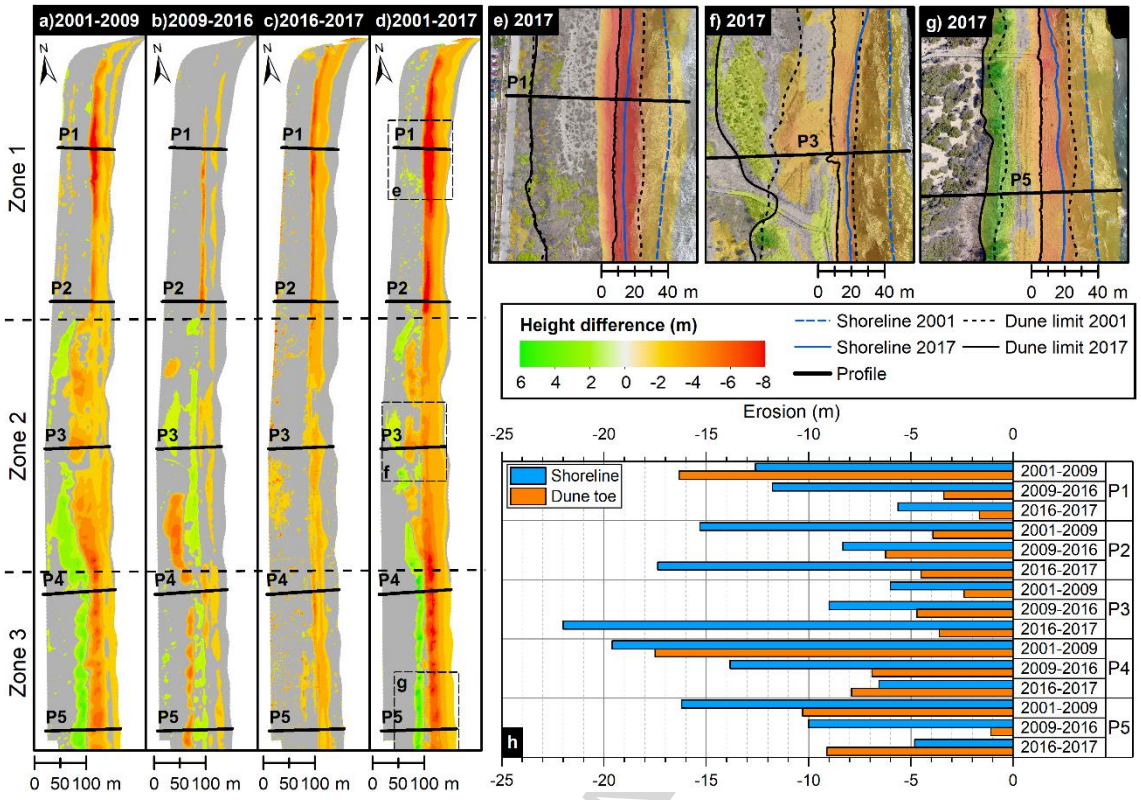

Figure 6: Height difference in each period (a-d). Plan view detail with the initial and final position of shoreline and dune limits marked (e-f). Shoreline and dune toe evolution in each profile (h).

Availability of high-resolution DEMs allows elevation changes to be detected with centimeter accuracy (Figure 6a-d). The stability threshold is 1.5 times RMSE Z, i.e. ±0.25 m. Thus, for the entire study period (2001-2017) the greatest changes occur in the beach and foredune, with erosion reaching a loss of up to 8 m in height in zone 1, detecting stability in the area near the road. Analyzing the changes by periods and zones, for the period 2001-2009 (Figure 6a) a significant erosion is detected in the entire coastal front. In zone 1 it is greater than in the rest, while in zones 2 and 3 both the loss and the increase in height are detected. This may indicate a shift towards the inland side of the dune, as variations in elevation are consistent. However, in the following period (Figure 6b) a change in the opposite direction is detected in these areas, due to the dune restoration works to fix the position of the foredune. In zone 1 erosion continues, although to a lesser extent than in the previous period. In the last available period

(Figure 6c) an increase of the generalized erosion is detected in the beach and the contiguous dune slope.

The variation in the position of the shoreline and the foot of the slope on the sea side of the dune has also been studied. A regression in both has been detected, being the shoreline in 2017 even behind the position of the dune boundary in 2001 (Figure 6e-g). This means an average sea advancement of 35.8 m. Analyzing the evolution by profiles and time periods (Figure 6h), some differences are detected in the different study areas. During the 2001-2009 period, the retreat of the shoreline was 2.5 times greater than at the foot of the dune, except for P1. In the following period this erosive rate was constant for the whole area, however in the 2016-2017 period the profiles located southwards (P4 and P5) suffered twice as much retreat in the dune as on the beach, while in those located to the north (P1 and P2) the situation is the opposite.

Figure 7 shows the most representative cross-shore transects that describe the changes that have occurred in the foredune and the beach. Profile P2 is in zone 1, at north, representing the most anthropized area with the artificial dune, which analysis is relevant since the date it was created (prior to 2001) and the material which is formed by. The Profile P5S also interesting because is located at the south, in zone 3, and can be shown the changes due to the restored of the foredune as well as the changes in the beach and the inner part of the dune.

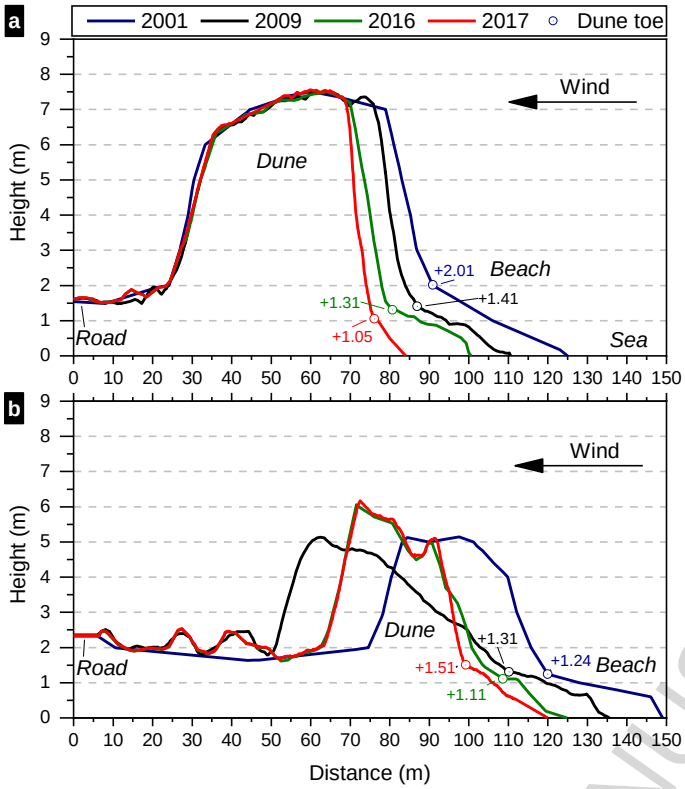

Figure 7: (a) Profile P2 in zone 1, artificial dune and (b) Profile P5 in zone 3, restored foredune.

In the artificial mound area, P2 (Figure 7a), the beach width falls from 34 m in 2001 to only 8 m in 2017. An increase in the slope of both the beach (disappearing the berm) and the dune is also detected. In addition, the evolution of the foot of the dune is remarkable. In this profile, the dune foot has experienced a retreat of 14.7 m and its height has decreased from 2.01 m to 1.05 m. In the case of profile P5 (Figure 7b) in 2001 and 2009 the dune profile had a natural profile formed by the wind, with the sea side (windward) having a more lain profile than the leeward side. A change in the position of the dune was detected between 2001 and 2009 without changing its shape, with a retreat of the shoreline similar to that of the dune toe (14 m vs 10 m) without changing its height. However, after the anthropogenic action, a narrower dune was generated, increasing its height by 1 m (2016 profile), which increased its slope angle. Erosion has caused the destruction of the beach berm in 2017 and a reduction of the dune base, destabilizing the slope at that point and causing loss of material.

3.2 Sedimentary budget

Supplementary data 5 summarizes the results by zones. A total of 143,561 m^3 of material was lost in the period 2001-2017. An increase in the erosion rates was detected in the last period. The overall annual loss rate was -8,517 m^3/year in the period 2001-2009, -2,785 m^3/year in the period 2009-2016 and -55,930 m^3/year in the period 2016-2017. The most affected area was zone 1, representing 55% of the total loss. Zone 2 accounts for 33% while zone 3 accounts for only 12%. This indicates that the further north and the nearer the mouth of the Segura river, the greater sediment loss is detected.

Analyzing the direction of the changes (supplementary data 5), the volume eroded in the dune is 1.5 times the beach erosion in 2001-2009 (-39,913 m^3, an annual rate of -4,989 m^3/year in dune whereas in the beach the loss was -28,223 m^3, an annual rate of -3,528 m^3/year). As stated before, this loss was greater at north (zone 1), decreasing towards south (zone 2 and 3). The relation between dune and beach erosion rates was: 2.3 for zone 1, 1.2 for zone 2 and 0.2 for zone 3. This trend continues in zone 1 for the period 2009-2016, where dune erosion was 1.8 times greater than beach erosion. However, in zone 2 the beach erosion was twice the dune loss and even the dune gained material in zone 3. Finally, the sediment loss in the last period (2016-2017) in both beach and dune was remarkable, being 20 times the erosion of the previous period and 7 times erosion rates from 2001-2009 period. Dune loss in zone 1 is -3,503 m^3/year further than beach erosion, while in zone 2 beach erosion prevails, with a loss of -9,971 m^3/year (-3,552 m^3/year of dune erosion). Sedimentary budget in zone 3 is similar between beach and dune, with a loss of -6,500 m^3/year in each dune and beach.

3.3 Sediment composition

According to sedimentology data obtained from the 2006 and 2017 sampling campaigns (Figure 8a), there is a generalized loss of fine-grained sediments (fine sand and silt fractions) throughout the study area. This loss has caused a significant increase in the median sediment

size (Figure 8b). The S4 sample stands out, which in 2006 was in the beach area with an median size of 0.301 mm (Figure 8d), while in 2017 it was -0.11 m below sea level with an median size of 0.396 mm (Figure 8e). Therefore, the erosion of the coast and the greater proximity of the sea have caused some of the fine-grained sediments to be dragged into the sea, so that the sand left on the beach and dune is gradually increasing its median size. This is also justified by the textural parameters obtained, which show a tendency towards symmetry of the sample (Figure 8i). In some samples a change in their median size and textural parameters is detected. For example, sample S3 (Figure 8b,c) or S8 (Figure 8f,g). Both are still on the crest of the dune. However, although they have not been affected by natural processes, they have been affected by human actions such as the reconstruction carried out in 2011.

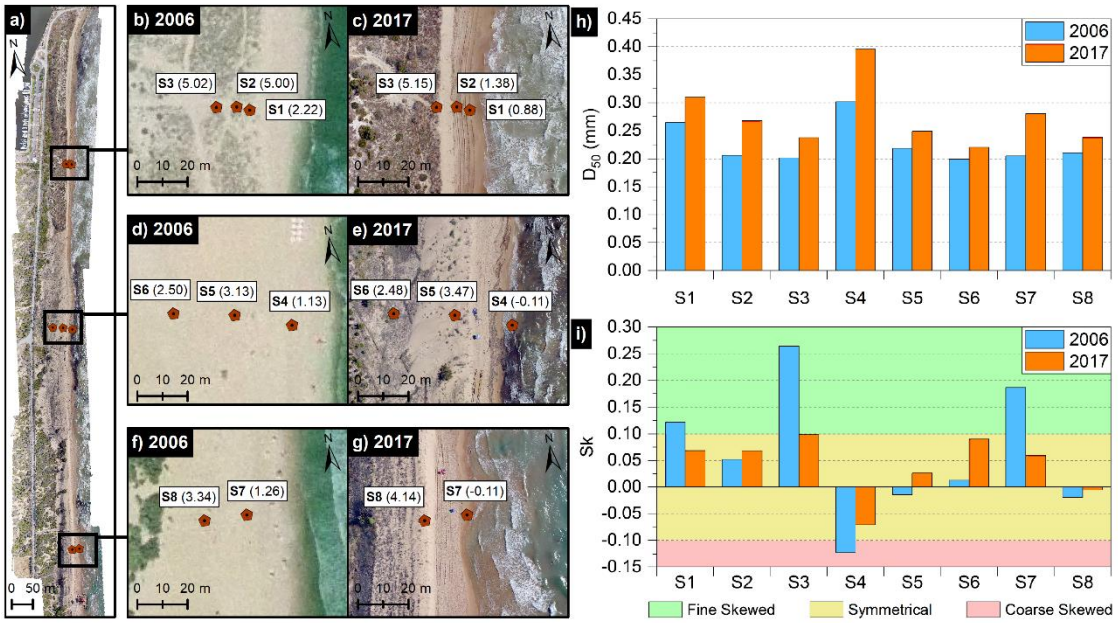

Figure 8: (a) Location of the sediment samples. (b,d,f) Detail of the location and height of the samples in 2006 and (c,e,g) in 2007. Note the change in height due to dune and beach erosion. (h) Median grain size D_{50}. (i) Skewness.

4 DISCUSSION

In coastal management, stablishing the sedimentary budget of a beach is fundamental in dune evolution studies (Hesp and Martínez, 2007). Transects that are perpendicular to the shore have been widely used to analyze coastal changes in the past (Bird, 1985; Dean, 1998; Dolan *et*

al., 1991), but currently accurate and repetitive DEM of the coast are needed for volumetric analysis (Scarelli *et al.*, 2017). GIS software platforms are widely used to analyze and visualize the spatial and temporal changes of the surface on coastal zones (Rodríguez *et al.*, 2009). They are an excellent tool for the to detect areas of sediment gain or loss by means of elevation data but there are also drawbacks that must be considered (Andrews *et al.*, 2002). Firstly, elevation datasets are based on points clouds which density vary from SfM-MVS photogrammetry from UAV (30 pts/m^2) , to LiDAR (0.5 pts/m^2) or GNSS-classical topography surveys (0.02 pts/m^2). The denser point cloud is, the more realistic 3D model of the surface can be obtained. Secondly, the conversion into a DEM/DSM are also relevant (Scarelli *et al.*, 2017). GIS usually uses two formats to work with elevation datasets, rasters datasets or TIN-based datasets. Raster datasets are grids where the height of each cell was determined by using the average height of all points falling in a grid cell and interpolates the voids. TIN-based datasets are a form of vector-based digital geographic data and are constructed by triangulating a set of vertices (points). The vertices are connected to a series of edges to form a network of Delaunay triangles. TINs are used for high-precision modeling because they allow more accurate calculations surface area and volume (Andrews *et al.*, 2002). Thus, in this research DEM/DSM input data was converted to ArcGIS Terrain datasets, detecting the changes over time with great precision and avoiding the uncertainties described by Elsner *et al.* (2018) of using raster elevation datasets to model the terrain.

This study also validates the use of aerial photogrammetry techniques using low take-off weight UAVs and their subsequent treatment with SfM-MVS algorithms for the generation of low cost and high quality DEMs (Supplementary data 2). The results are comparable to those obtained Scarelli *et al.* (2017) and Elsner *et al.* (2018). Although in our research the average vertical RMSE is the double (0.173 m vs 0.08 m), our area of study is larger and more complex, with RMSE over dune zone similar to the obtained by them. In addition, the precision obtained by the 3D model via UAV (Figure 5) is below the maximum error allowed for LiDAR flights

(RMSE XY < 0.3 m and RMSE Z < 0.2 m, (PNOA, 2009; PNOA, 2016)), and the density of the point cloud points obtained is much higher (30 pt/m^2 vs 0.5 pt/m^2) (Supplementary data 3 and 4). This allows highly detailed modeling of the complex shapes of dune systems, as well as the detection of changes and the calculation of sediment volumes with greater precision. Fieldwork is also less time-consuming than classical surveying methods and costs less than LiDAR flights or vehicle mounted laser scaners, which means that UAVs are a viable, low cost and flexible alternative to laser scanning approaches, as Elsner *et al.* (2018) state. This makes it possible to monitor the study area more frequently, conducting control campaigns every 6 months or after storm events. The main disadvantage of this technique involves the issue of accurately processing shrub zones. The presence of vegetation on foredunes affects the photogrammetric reconstruction of the terrain, and if not masked its seasonal changes may generate a spatial difference that can be considered as a volume change in the measurements obtained by the difference surface tool (Scarelli *et al.*, 2017). In this work the vegetation cover has been manually masked, but there are algorithms and filtering techniques to automatically identify the vegetation and create DSM instead of DEM (Gupta *et al.*, 2018).

The results obtained show that the highest beach erosion occurs in zone 1, the area close to the Segura river mouth. In contrast, the loss in zone 3 is the lowest during all periods. This erosion is a consequence of the cut-off of longitudinal sediment transport caused by the breakwaters at the Segura River mouth (Aragonés *et al.*, 2016). In the present work an increase in the erosive rate in the period 2016-2017 was detected (Figure 6h), confirming the results already identified by Pagán *et al.* (2017). This continuous retreat of the shoreline has allowed to the sea to reach the dune, causing its erosion. In the period 2001-2009, before the dune restoration, erosion mainly affect at the beach. In zone 1 the mound is fixed, so the dune loss is only consequence of the erosion of the beach, but in zones 2 and 3 the dune moved inland and scarcely loss sediment (Figure 6a). To prevent that the movement of the dune in zones 2 and 3 affected the road, in 2011 the restoration of the foredune was executed.

The first elevation data available after dune reconstruction is 2016 LiDAR survey, but the effects of the restoration can be appreciated (Figure 6b) such as the increase in the volume of the dune (Supplementary data 5). In zone 1 the dredged material was not removed, maintaining the artificial mound, against the projected solution noted in section 2.3. In zones 2 and 3 the projected criteria was to fix the dune in its position, maintaining its natural height and slopes (MAPAMA, 2001). However, a dune shift towards the sea and an increase in elevation of more than 1 m was detected in these zones (Figure 6b and Figure 7b). During the time span between the development of the restoration project and its execution (10 years) the backshore receded 18 m, which possibly resulted in modifications during the execution of the restoration project, establishing new objectives: (i) to maintain the backshore width as far as possible, and (ii) to preserve the width of the dune (Figure 7b). This occasioned the reconstruction of the foredune closer to the shoreline with steeper slopes, eliminating the protection of the beach berm. The lack of enough backshore width could have led to the increase of the erosion detected in the last period (2016-2017).

Indeed, wave attack at the dune foot steepens the dune profile which may collapse by avalanching. Wave attack may also create a notch at the dune foot leading to mass failure: collapse of a dune slab. That could also explain the steeper slope observed in the seaward side of the coastal dune (Figure 7, and Figure 9a-b). The existing beach in 2017 was a dune area in 2001 (Figure 7e-g). Visually, this erosive phenomenon is identified in the stairs leading to the beach and in the fence that delimited the dune foot (Figure 9c,d).

Although no relevant differences have been detected in the storms during the study period, the coincidence of 4 storms in a few months, together with the almost complete elimination of the beach berm, are undoubtedly responsible for a significant loss of volume of the dune in the period 2016-2017 (Supplementary data 5). The diverse composition of the sedimentary materials forming the different areas of the foredune also had influence on the erosion rates.

The results of the granulometric analysis show a generalized increase in the mean grain size D_{50} along the study period. This increase in grain size is due to the washing of fine-grained sediments once the sea has reached the dune foot (Figure 8). Moreover, it has been found that the mound in zone 1 is formed by sandy silts (Figure 9g), which favors its cross-shore transport to the off-shore zone, as proved in the study from López *et al.* (2019). Precisely zone 1 suffers the greatest sediment loss (47,808 m^3, 23.5% of its initial volume).

Figure 9: Mosaic with representative images. (a) Dune toe eroded in zone 3. (b) Slope of the artificial dune in zone 1, with the toe eroded and landslides due to regrading. (c) Erosion of the dune, the fence marked the dune toe in 2007. (d) Foundation of the wooden walkway in the air due to erosion. (e) View of vegetation on dune in 2015 and (f) in 2017. Note the loss of vegetation. (g) Layers of silt and debris on the artificial dune in zone 1. (h) Dry trees due to shoreline erosion. (i) View of the state of vegetation on the foredune in zone 2.

Apart from the erosive coastal dynamics mentioned above, the effect of anthropogenic actions on the foredune must be added. For example, the continuous process of regrading the seaside slope of the dune. As the foot of the dune is undermined, detachments of material from its upper part frequently occur (Figure 9b). In order to prevent these landslides from affecting the users, the manager re-lighted the slope, although according to what has been detected in this

study, the slope is much steeper than the angle of internal friction of the soil (Figure 5e-h). Moreover, the dune profile is frequently altered by the frequent machinery operation for cleaning the beach (Figure 9a). This process usually moves sand from the dune to the beach in order to widen the berm for beach users but forming a much more steeped slope in the seaward side of the dune (Figure 8). In addition, the high resolution of the images taken allows to observe the footsteps of beach users crossing the dune, identifying the users' desire paths to access the beach (Figure 4). The simple fact that people cross the dune to go to the beach can cause a strong impact, as it tends to fragment the foredune by creating corridors, which in turn increase the erosive action of the wind, leading to the formation of gaps in the foredune that increase its vulnerability (Ley *et al.*, 2007). The coast manager could use this information to effectively project access paths through the areas actually used by beach users. This measure would prevent the breaking of the protective fence by the users and the consequent affection to the dune vegetation (Figure 9i).

It is therefore necessary to take appropriate action to protect the shoreline from the degradation processes detected. Considering the increase in the erosive rates detected in the last study period (-11.2 m/year shoreline, -5.32 m of dune foot, -44,298 m^3 of lost material), only 7 years would be necessary for the complete elimination of the foredune.

CONCLUSIONS

This work has validated the use of UAV to obtain a high-precision 3D model of the dune and beach surface using photogrammetry-based SfM-MVS algorithm. It is a fast, reliable and highly accurate technique that allows to model complex and changing environments, such as dune ecosystems, at lower costs than LIDAR surveys. Furthermore, this research shows that it is possible to analyze the evolution of these systems on a regular and detailed basis, either through new UAV flights or by integrating pre-existing cartographic information into GIS platforms.

This study has detected an increase in the erosion of the study area. A total of 143,561 m^3 of sediment has been lost in the period 2001-2017. The retreat of the shoreline at rates higher than 2.5 m/year has caused the decrease of backshore width by 53%. This reduction has led to the disappearance of the beach berm and a lowering of the foot of the dune slope of up to 1 m. Thus, the storms can reach the dune more easily, increasing the erosion and destabilization of the seaward slope. This progressive advance of the sea has also generated an increase in the median grain size of the sediments due to the washing fine sand and silt fractions. Moreover, it has been confirmed that the restoration works have not had the desired effect. As a consequence of the reduction in the available space, a narrower and higher dune was created with slopes steeper than natural ones, increasing the risk of landslides and the loss of material.

In conclusion, this work contributes to improving the knowledge of the pressures on the coastal dunes system and the behavior of natural and restored dunes due to these pressures. The method presented in this research, based on the use of photogrammetry from UAV and GIS techniques, provides a high-resolution DSM, which can be compared with previous surveys to obtain accurate measurements of volumetric sediment changes in coastal environments. Therefore, due to its flexible deployment, it could be used by coastal managers to regularly monitor the threatened dune-beach systems so they can take the appropriate decisions for their adequate preservation.

REFERENCES

Agisoft 2016. Agisoft PhotoScan Professional Edition.

Aldeguer, M., 2008. Indicadores ecológicos como elementos de soporte del acto administrativo de deslinde de la zona marítimo terrestre. Universidad de Alicante, Master's thesis, p.

Andrews, B.D.; Gares, P.A., and Colby, J.D., 2002. Techniques for GIS modeling of coastal dunes. *Geomorphology,* 48(1–3), 289-308.

Aragonés, L.; Pagán, J.I.; López, M.P., and García-Barba, J., 2016. The impacts of Segura River (Spain) channelization on the coastal seabed. *Science of The Total Environment,* 543, 493-504.

Bird, E.C.F. 1985. *Coastline changes. A global review,* United States, John Wiley and Sons Inc., New York, NY.

Burak, S.; Dog˘An, E., and Gaziog˘Lu, C., 2004. Impact of urbanization and tourism on coastal environment. *Ocean & Coastal Management,* 47(9–10), 515-527.

Carter, R.; Hesp, P., and Nordstrom, K., 1990. Erosional landforms in coastal dunes. *Coastal Dunes: form and process*, 217-250.

Chen, B.; Yang, Y.; Wen, H.; Ruan, H.; Zhou, Z.; Luo, K., and Zhong, F., 2018. High-resolution monitoring of-Beach topography and its change using unmanned aerial vehicle imagery. *Ocean and Coastal Management,* 160, 103-116.

Colomina, I. and Molina, P., 2014. Unmanned aerial systems for photogrammetry and remote sensing: A review. *Journal of photogrammetry remote sensing,* 92, 79-97.

Dandois, J.P. and Ellis, E.C., 2010. Remote sensing of vegetation structure using computer vision. *Remote Sensing,* 2(4), 1157-1176.

Dean, R.G., 1998. Beach nourishment: a limited review and some recent results. *Proceedings of the 26th International Conference on Coastal Engineering* (Copenhagen, Denmark), pp. 45-69.

Delacourt, C.; Allemand, P.; Jaud, M.; Grandjean, P.; Deschamps, A.; Ammann, J.; Cuq, V., and Suanez, S., 2009. DRELIO: An unmanned helicopter for imaging coastal areas. *Journal of Coastal research*, 1489-1493.

Dolan, R.; Fenster, M.S., and Holme, S.J., 1991. Temporal analysis of shoreline recession and accretion. *Journal of coastal research*, 723-744.

Drummond, C.D.; Harley, M.D.; Turner, I.L.; A Matheen, A.N., and Glamore, W.C., 2015. UAV applications to coastal engineering. *Proceedings of the Australasian Coasts & Ports Conference 2015: 22nd Australasian Coastal and Ocean Engineering Conference and the 15th Australasian Port and Harbour Conference*, pp. 267.

Ecolevante 2006. *Estudio ecocartográfico del litoral de las provincias de Alicante y Valencia*, Dirección General de Costas, Ministerio de Medio Ambiente, Spain, [Available online: http://www.mapama.gob.es/es/costas/temas/proteccion-costa/ecocartografias/ecocartografia-alicante.aspx].

Elsner, P.; Dornbusch, U.; Thomas, I.; Amos, D.; Bovington, J., and Horn, D., 2018. Coincident beach surveys using UAS, vehicle mounted and airborne laser scanner: Point cloud inter-comparison and effects of surface type heterogeneity on elevation accuracies. *Remote Sensing of Environment,* 208, 15-26.

Esri 2016. ArcGIS Desktop 10.5.

Gonçalves, J. and Henriques, R., 2015. UAV photogrammetry for topographic monitoring of coastal areas. *ISPRS journal of Photogrammetry and Remote Sensing,* 104, 101-111.

Gupta, A.; Byrne, J.; Moloney, D.; Watson, S., and Yin, H., 2018. Automatic Tree Annotation in LiDAR Data. *Proceedings of the GISTAM*, pp. 36-41.

Halpern, B.S.; Kappel, C.V.; Selkoe, K.A.; Micheli, F.; Ebert, C.M.; Kontgis, C.; Crain, C.M.; Martone, R.G.; Shearer, C., and Teck, S.J., 2009. Mapping cumulative human impacts to California Current marine ecosystems. *Conservation Letters,* 2(3), 138-148.

Hesp, P.A. and Martínez, M.L., 2007. Disturbance processes and dynamics in coastal dunes. *Plant disturbance ecology: the process and the response*, 215-247.

Jaakkola, A.; Hyyppä, J.; Kukko, A.; Yu, X.; Kaartinen, H.; Lehtomäki, M., and Lin, Y., 2010. A low-cost multi-sensoral mobile mapping system and its feasibility for tree measurements. *ISPRS journal of Photogrammetry and Remote Sensing,* 65(6), 514-522.

Javernick, L.; Brasington, J., and Caruso, B., 2014. Modeling the topography of shallow braided rivers using Structure-from-Motion photogrammetry. *Geomorphology,* 213, 166-182.

Komar, P.D. 1983. Nearshore currents and sand transport on beaches. *Elsevier oceanography series.* Elsevier.

Ley, C.; Gallego-Fernández, J.B., and Vidal, C. 2007. Manual de restauración de dunas costeras. *Ministerio de medio ambiente.*

Long, N.; Millescamps, B.; Guillot, B.; Pouget, F., and Bertin, X., 2016. Monitoring the topography of a dynamic tidal inlet using UAV imagery. *Remote Sensing,* 8(5), 387.

López, M.; Baeza-Brotons, F.; López, I.; Tenza-Abril, A.J., and Aragonés, L., 2019. Factors influencing the rate of beach sand wear: Activation layer thickness and sediment durability. *Science of The Total Environment,* 658, 367-373.

Lucieer, A.; Jong, S.M.D., and Turner, D., 2014. Mapping landslide displacements using Structure from Motion (SfM) and image correlation of multi-temporal UAV photography. *Progress in Physical Geography,* 38(1), 97-116.

Mancini, F.; Dubbini, M.; Gattelli, M.; Stecchi, F.; Fabbri, S., and Gabbianelli, G., 2013. Using unmanned aerial vehicles (UAV) for high-resolution reconstruction of topography: The structure from motion approach on coastal environments. *Remote Sensing,* 5(12), 6880-6898.

Mapama 2001. Recuperación del ecosistema dunar de Guardamar del Segura, tramo Casas de Babilonia – Desembocadura del río Segura (Alicante). *In:* COSTAS, D.G.D. (ed.).

Mapama. 2017. *Galería de imágenes* [Online]. Madrid, Spain: Gobierno de España. Available: http://www.mapama.gob.es/es/prensa/galeria-de-imagenes/ [Accessed 21/03/2017 2017].

Matarredona Coll, E.; Marco Molina, J.A., and Prieto Cerdán, A., 2006. La configuración física del litoral sur alicantino.

Miřijovský, J. and Langhammer, J., 2015. Multitemporal monitoring of the morphodynamics of a mid-mountain stream using UAS photogrammetry. *Remote Sensing,* 7(7), 8586-8609.

Mitasova, H.; Overton, M., and Harmon, R.S., 2005. Geospatial analysis of a coastal sand dune field evolution: Jockey's Ridge, North Carolina. *Geomorphology,* 72(1–4), 204-221.

Niethammer, U.; James, M.; Rothmund, S.; Travelletti, J., and Joswig, M., 2012. UAV-based remote sensing of the Super-Sauze landslide: Evaluation and results. *Engineering Geology,* 128, 2-11.

Pagán, J.I.; Aragonés, L.; Tenza-Abril, A.J., and Pallarés, P., 2016. The influence of anthropic actions on the evolution of an urban beach: Case study of Marineta Cassiana beach, Spain. *Science of The Total Environment,* 559, 242-255.

Pagán, J.I.; López, I.; Aragonés, L., and García-Barba, J., 2017. The effects of the anthropic actions on the sandy beaches of Guardamar del Segura, Spain. *Science of The Total Environment,* 601-602, 1364-1377.

Pix4d 2019. Pix4Dcapture.

Pnoa 2009. Especificaciones Técnicas para VUELO FOTOGRAMÉTRICO DIGITAL con VUELO LIDAR. *In:* NACIONAL, I.G. (ed.).

Pnoa 2016. Especificaciones Técnicas para VUELO FOTOGRAMÉTRICO DIGITAL con VUELO LIDAR. *In:* NACIONAL, I.G. (ed.).

Prosdocimi, M.; Calligaro, S.; Sofia, G.; Dalla Fontana, G., and Tarolli, P., 2015. Bank erosion in agricultural drainage networks: new challenges from structure-from-motion photogrammetry for post-event analysis. *Earth Surface Processes and Landforms,* 40(14), 1891-1906.

Revell, D.L.; Komar, P.D., and Sallenger Jr, A.H., 2002. An application of LIDAR to analyses of El Niño erosion in the Netarts Littoral Cell, Oregon. *Journal of Coastal Research*, 792-801.

Rodríguez, I.; Montoya, I.; Sánchez, M.J., and Carreño, F., 2009. Geographic Information Systems applied to Integrated Coastal Zone Management. *Geomorphology,* 107(1–2), 100-105.

Sallenger Jr, A.; Krabill, W.; Swift, R.; Brock, J.; List, J.; Hansen, M.; Holman, R.; Manizade, S.; Sontag, J., and Meredith, A., 2003. Evaluation of airborne topographic lidar for quantifying beach changes. *Journal of Coastal Research*, 125-133.

Scarelli, F.M.; Cantelli, L.; Barboza, E.G.; Rosa, M.L.C., and Gabbianelli, G., 2016. Natural and Anthropogenic coastal system comparison using DSM from a low cost UAV survey (Capão Novo, RS/Brazil). *Journal of Coastal Research,* 75(sp1), 1232-1237.

Scarelli, F.M.; Sistilli, F.; Fabbri, S.; Cantelli, L.; Barboza, E.G., and Gabbianelli, G., 2017. Seasonal dune and beach monitoring using photogrammetry from UAV surveys to

apply in the ICZM on the Ravenna coast (Emilia-Romagna, Italy). *Remote Sensing Applications: Society and Environment,* 7, 27-39.

Snavely, N.; Seitz, S.M., and Szeliski, R., 2008. Modeling the World from Internet Photo Collections. *International Journal of Computer Vision,* 80(2), 189-210.

Steffen, W.; Crutzen, P.J., and Mcneill, J.R., 2007. The Anthropocene: Are Humans Now Overwhelming the Great Forces of Nature. *AMBIO: A Journal of the Human Environment,* 36(8), 614-621.

Stockdon, H.F.; Doran, K.S., and Sallenger Jr, A.H., 2009. Extraction of lidar-based dune-crest elevations for use in examining the vulnerability of beaches to inundation during hurricanes. *Journal of Coastal Research*, 59-65.

Turner, I.L.; Harley, M.D., and Drummond, C.D., 2016. UAVs for coastal surveying. *Coastal Engineering,* 114, 19-24.

Woolard, J.W. and Colby, J.D., 2002. Spatial characterization, resolution, and volumetric change of coastal dunes using airborne LIDAR: Cape Hatteras, North Carolina. *Geomorphology,* 48(1-3), 269-287.

Highlights

- UAVs are used to monitor dune changes
- High-precision 3D model of the dune system was created using SfM-MVS algorithm
- Sediment balance of the dune-beach system was analyzed using GIS techniques
- A loss of 143,561 m^3 of material from 2001 to 2017 was detected
- The anthropic pressure increases the dune and beach erosion.